Title
A model of high resolution cross strip readout for photon and ion counting imaging detectors

Journal
IEEE Transactions on Nuclear Science, 52(5)

ISSN
0018-9499

Authors
Tremsin, A S
Siegmund, OHW
Vallerga, J V

Publication Date
2005-10-01

Peer reviewed

A Model of High Resolution Cross Strip Readout for Photon and Ion Counting Imaging Detectors

Anton S. Tremsin, Oswald H. W. Siegmund, John V. Vallerga

Abstract--Recent advances in the photon counting, imaging readout for microchannel plate (MCP) detectors has led to a substantial improvement in their spatial resolution. The spatial accuracy (~7-10 μm) of an MCP detector with a cross strip readout has been shown to be limited by the MCP pore size (<10 μm). In this paper we study the ultimate resolution limits of the cross strip readout itself. The model allows us to determine the requirements on the anode's geometry and the signal processing electronics in order to reach a particular spatial resolution. The optimal detector parameters, such as the width of the charge footprint at the anode (determined by the distance and the field between the MCP and the anode), and the gain of the detector can also be found with the help of our model. The model indicates that the optimum FWHM of the charge footprint distribution at the anode is a factor of ~1.6 larger than the anode period. Given a noise of charge sensitive amplifiers of 350 electrons rms each we predict that the MCP gain can be as low as 2.5×10^5 for this detector to resolve ~7 μm features.

Results of our modeling also indicate that the accuracy of the position obtained for center of gravity centroiding of the charge distribution is inferior to fitting a Gaussian-like analytical function, providing the geometry of the anode is accurate enough. The model predictions are compared with the experimentally measured images and reveal the critical parameters (anode's geometricaccuracy and amplifier noise), which can be improved in future detectors.

***Index Terms*—Position sensitive detectors, Photon detectors, Image resolution.**

I. Introduction

THE cross strip (XS) anode is a high resolution (~5 μm) charge division readout used in photon counting imaging detectors with microchannel plates [1]-[3]. The anode has a coarse (~0.5 mm) multi-layer metal and ceramic cross strip pattern on a ceramic (alumina) substrate. The charge from a microchannel plate stack is divided between two orthogonal sets of strips. Each strip of the anode is connected to a low noise charge sensitive amplifier followed by subsequent analog to digital conversion of individual strip charge values. The event position is determined from the measured charges by centroiding. The coarse position of the registered photon or particle corresponds to the center peak of the charge cloud, while the charge cloud centroid can be calculated to a small fraction of the strip period (currently to ~1%) by an appropriate software or hardware algorithm. In the simplest case the centroid is just the weighted sum of the strip charges. Fitting an analytical function corresponding to the charge distribution (e.g. non-linear Gaussian fit) can result in higher accuracy of centroiding. The measured resolution of our current cross strip readout and its associated electronics is on the scale of the MCP pore dimension (~6-10 μm) and is not limiting the spatial resolution of the detector. However, the discrete nature of the event detection by an MCP will not be a limiting factor when microchannel plates with smaller pore sizes (down to 2 μm) become widely available. The resolution of the XS readout can then be further improved in order to match the ~ 2 μm resolution limit due to the MCP geometry. Besides that, the linearity of the existing anode does not match its spatial resolution capabilities. The fixed-pattern (and therefore correctable by appropriate calibration) image distortions are currently larger than the anode's spatial resolution.

We have developed a model of the interaction of the MCP charge cloud with the cross strip anode and its associated electronics including the centroiding algorithms. For a given charge cloud distribution at the plane of the XS anode, the ideal charge values are calculated for each anode electrode by the numerical integration of the charge distribution over the area of each electrode. Subsequently the charges corresponding to electronic noise (generated by a random number generator in accordance with the given noise distribution) are added to each electrode and the resulting arrays of charge values are passed to a centroiding algorithm. This process is repeated for each individual photon. With the help of this model, described in this paper, we have localized the source of XS anode distortions and subsequently have improved the anode's manufacturing process in order to meet the linearity requirements. We also use the model to determine the detector operational parameters (such as the charge footprint dimension, and MCP gain versus the noise of charge sensitive amplifiers) in order to achieve a given spatial resolution.

Manuscript received October 12, 2004.

This work was supported by NASA grant #NAG5-11394

The authors are with Experimental Astrophysics Group, Space Sciences Laboratory, University of California, Berkeley, California 94720, USA (telephone: 510-642-4554, e-mail: ast@ssl.berkeley.edu).

II. Model Description

In our model the charge footprint on the anode is approximated by a best fit of Gaussian function to the experimentally measured charge distribution, which was found to be very close to a Gaussian [4],[5]. For each modeled photon with position (X_{ph},Y_{ph}) relative to the anode the charge is divided between the electrodes of the cross strip anode. The value of charge at each finger is determined by a numerical integration of charge distribution over the area of the electrode. Subsequently, a charge variation corresponding to the electronic noise of charge sensitive amplifiers is added/subtracted to the charges in each strip. The noise is generated in accordance with the normal distribution for a given rms value by a random number generator. The two arrays of resulting charges are passed to a centroiding algorithm, which recovers the event coordinates (X_c,Y_c) from the given charge values. The process is repeated for a given number of photon events with coordinates ($X_{ph}Y_{ph}$) distributed over the modeled image area.

Strictly speaking this algorithm simulates only top electrodes of XS anode, which comprise a set of continuous electrodes, while the bottom electrodes are shadowed by the top fingers and therefore for the electron collection effectively consist of interrupted set of rectangles. Although the present model is developed primarily for top electrodes of XS anode, it still can be applied to the bottom electrodes, providing the width of top electrodes is small enough. Our experimental data, indicating that the spatial resolution achievable with both top and bottom electrodes is effectively the same, confirms the latter statement.

Full field illumination images were used to study the linearity and resolution of the XS anode itself. The full field illumination of the detector was represented in our model by photon positions ($X_{ph}Y_{ph}$) corresponding to the centers of micropores (hexagonally packed for the circular pore geometry). The resulting images were compared to the experimentally obtained images, where individual pores were resolved [1],[2].

The other type of images used in our modeling represented a section of standard US Air Force (USAF) resolution mask (Group 5, elements 1-6 and Group 6, elements 1 and 2). These images represent the detector spatial resolution for a given set of parameters and can also be compared with the previously obtained experimental data [3] for the verification of the model.

III. Modeling Results

A. *Width of the Charge Footprint*

The width of the charge cloud footprint at the plane of the anode obviously has to be optimized in order to achieve the highest resolution. Indeed, a too narrow footprint results in an under-sampled charge distribution. At the same time too wide charge footprint leads to charge division between large number of anode electrodes and consequently to the reduction of signal-to-noise ratio (especially at the edge of the charge distribution) leading to the resolution degradation. We investigated how sensitive is the detector resolution to the variation of the charge footprint. First the error of recovered photon coordinate X_c was calculated as a function of photon position X_{ph}. In these calculations we assumed that there is no electronic noise, thus only the effect of anode sampling function influenced the resolution. Fig. 1 shows the calculated error (X_c - X_{ph}) as a function of X_{ph}. The error of recovered photon position is obviously a periodic function with the period equal to the period of the anode. The legend indicates the value of charge footprint widths (FWHM of Gaussian distribution, in units of anode period) for each calculated curve.

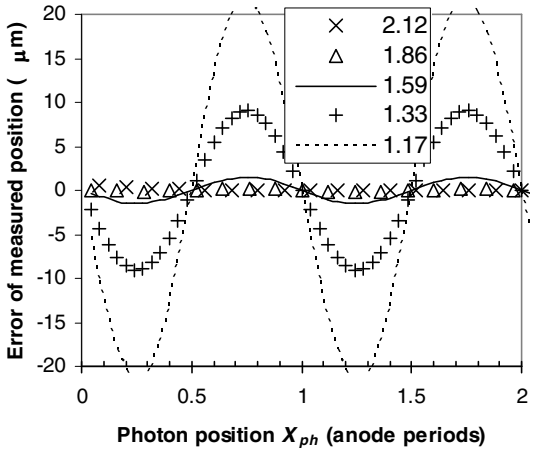

Fig. 1. The predicted error of the measured photon centroid X_c as a function of photon incidence coordinate X_{ph}, calculated for different charge footprint widths. The value of charge footprint FWHM (in units of anode period) is shown in the legend. No electronic noise is taken into account in calculations. Charge footprint is approximated by a Gaussian function. XS anode electrodes are 0.2 mm wide on 0.5 mm period.

The maximum error as a function of charge footprint width is shown in Fig. 2 for three different widths of anode electrodes (the period of anode - P_{anode} is the same). It is seen from Fig. 2 that the charge footprint FWHM cannot be smaller than ~1.6 P_{anode} for the sampling function not to limit the detector resolution. In case the amplifiers' noise is not negligible the error will increase more rapidly for footprint FWHM >2 P_{anode} then the curves shown in Fig.2, calculated for zero noise amplifiers. For the calculations described in the following sections the width of the charge footprint FWHM was chosen to be equal to 1.6 P_{anode} (in agreement with our experimental conditions [3]). The footprint width of 1.6 P_{anode} was found to be optimal as a narrower charge footprint would be undersampled (as seen from Fig. 2) and a wider footprint would have smaller signal-to-noise ratio, leading to degradation of spatial resolution.

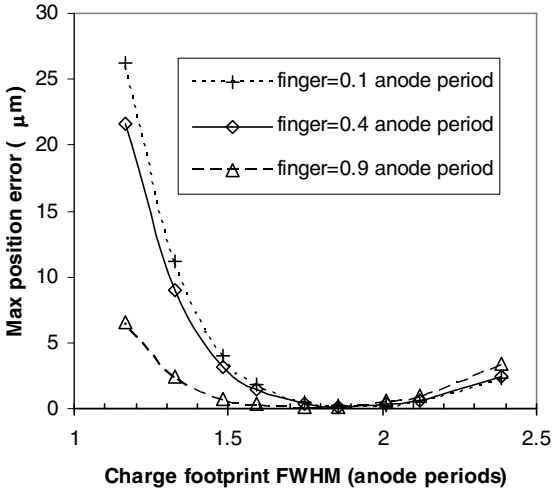

Fig. 2. The predicted maximum error of measured photon position X_c as a function of charge footprint size. Three curves represent different widths of anode fingers for the same anode period of 0.5 mm: crosses – 50 μm, diamonds – 200 μm and triangles – 450 μm wide electrodes, respectively. No electronic noise is taken into account.

B. Electronic Noise of Charge Sensitive Amplifiers and Detector Gain

The noise in the charge-sensing amplifiers is one of the most important parameters of the detector determining the accuracy of the cross strip anode position encoding. Defining the level of acceptable noise in the amplifiers for a given detector spatial resolution can be very useful for the selection and design of the signal processing electronics. Not only the spatial accuracy of the detector can be predicted, but also the counting rate capabilities are influenced by the selection of a particular set of amplifiers. Indeed, the minimum time required for the processing of a single event cannot be smaller than the peaking time of the charge amplifiers. Generally it takes longer to measure the charge with better accuracy (less noise) and therefore the dead time of the detector increases with the reduction of the electronic noise. The images generated with the help of our model for different levels of amplifier noise are shown in Fig. 3. In these calculations the input to the detector corresponded to an image mask with a set of dark/white line pairs.

The hexagonal pattern seen in Fig. 3.a corresponds to the hexagonal MCP pore geometry (4 μm pore-to-pore spacing), which is resolved at electronic noise of 200 e rms and detector operating at gain of 5×10^5. Each spot in this image represents a single pore, indicating that the spatial resolution of the XS anode better than 4 μm. In the ideal case the image of each pore is a point, but the presence of noise and discreteness of measured charge distribution determines the width of a pore image. As seen from Fig. 3, the spatial resolution of the detector degrades as noise is increased. The finest lines (71.8 line pairs per millimeter) are not resolved at noise larger than 700 e. Cross sections through the same groups of lines on the images illustrate the level of modulation for these sets of line pairs, Fig. 4.

The high frequency oscillations in Fig. 4.a correspond to single pores on 4 μm period being resolved by the anode. It is obvious that in order to resolve the smallest features in this image mask (7 μm wide lines) the detector gain can be further decreased if electronic noise is below 500 e (the advantages of low gain operation are emphasized in our previous papers [2],[3] and references therein). In general it is the value of the ratio of detector gain to the electronic noise which should be considered as a parameter defining the limit of spatial resolution of the detector. In theory the gain of our existing detectors with XS anode can be increased so that the spatial resolution will match the geometry of emerging small pore (~2 μm) MCPs. The dynamic range of charge sensitive amplifiers, however, sets up the upper limit of detector gain for a given value of electronic noise.

The modeled images can be compared to experimentally obtained image of USAF resolution mask shown in Fig. 5. The cross sections through the element 1 of Group 6 in this image correspond to the middle three peaks in cross sections of Fig. 4.b (64 line pairs per millimeter). The agreement between the modeled and measured data proves the accuracy of our model. The distortions seen in the Fig. 5 are due to some inaccuracy of finger geometry in our first XS anodes, discussed in the next section.

Providing the accuracy of the anode geometry is adequate (see next section), the spatial resolution of the detector can be improved by application of more efficient centroiding algorithms, discussed in detail in references [6]-[8].

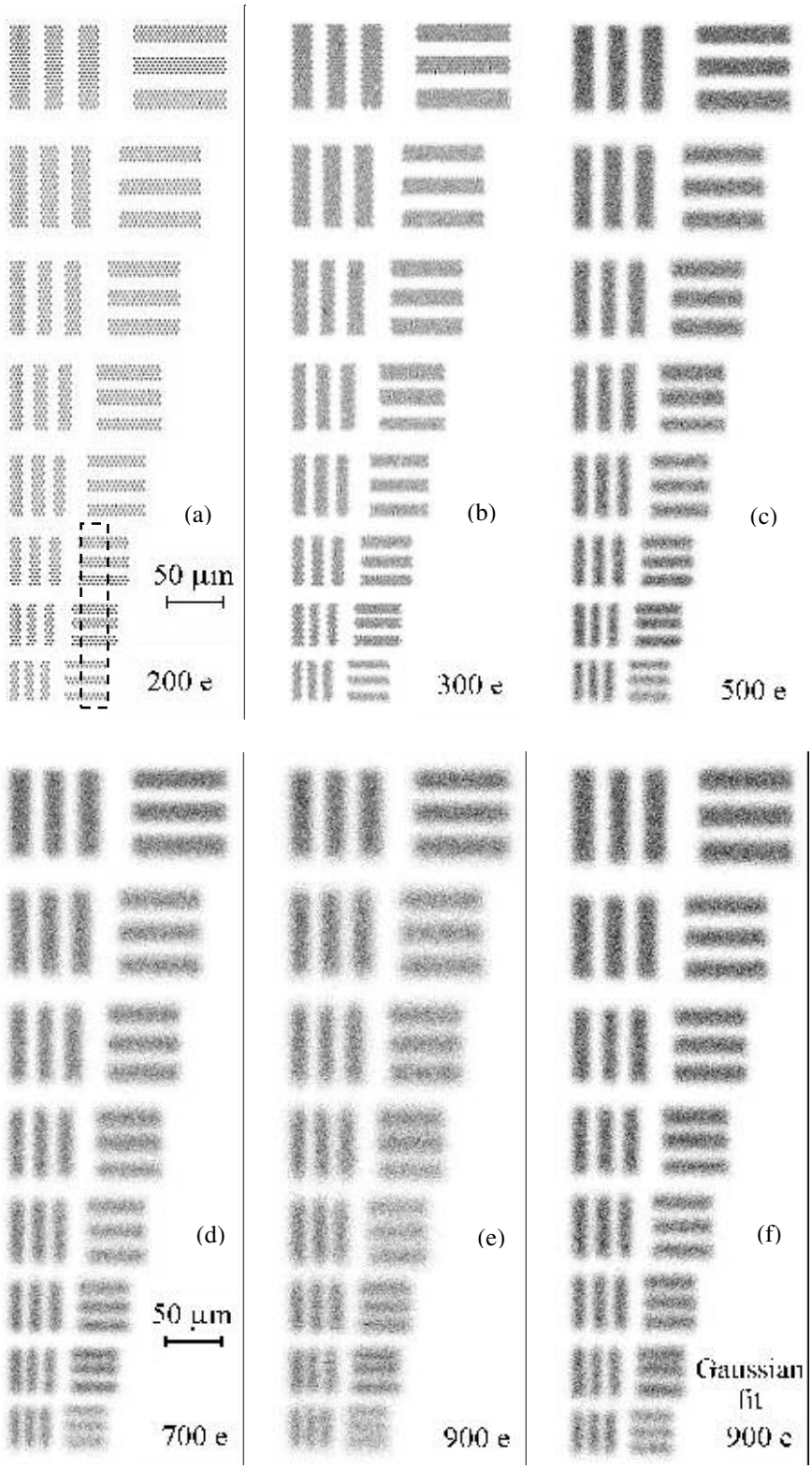

Fig. 3. Predicted resolution mask images obtained with different level of noise in charge sensitive amplifiers: 200, 300, 500, 700 and 900 electrons rms. The image mask has groups of 32, 36, 40.3, 45.3, 50.8, 57, 64 and 71.8 line pairs per mm, corresponding to Group 5 (elements 1-6) and Group 6 (elements 1 and 2). The mask was positioned in front of an MCP with hexagonally packed pores on 4 μm period. Calculation of photon position X_c is done with the center of gravity algorithm, except for the image (f), where Gaussian fit to charge distribution was used. XS anode geometry: anode period is 0.5 mm; top and bottom fingers are 0.2 mm and 0.45 mm wide, respectively. Image of each MCP pore has 500 modeled photons. Charge footprint assumed to be a Gaussian function with FWHM of 1.6 anode period. Detector gain is assumed to be 5×10^5. The cross sections through the same position in all images indicated by a dashed rectangle in (a) are shown in Fig. 4.

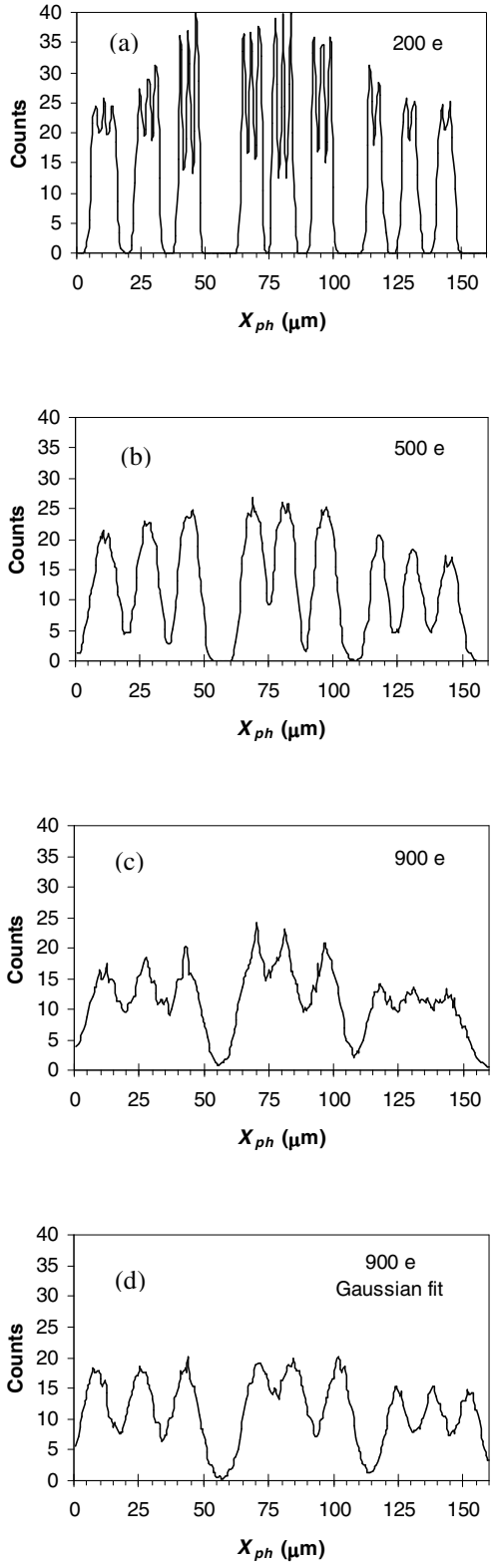

Fig. 4. Cross-sections through the images (a), (c), (e) and (f) of Fig. 3 taken at the same position, shown in the image of Fig3.a. The 3 sets of peaks in these cross sections correspond to 57, 64 and 71.8 line pairs per mm. The electronic noise for each image is shown in the legend. Individual pores on 4 μm centers are resolved in cross-section (a).

The cross sections shown in Figs. 4.c and 4.d, correspond to center of gravity and Gaussian fit centroiding algorithms respectively applied to the same detector data (anode geometry was assumed to be perfect in these calculations). The Gaussian fit centroiding resolved the smallest features on the mask (71.8 line pairs per mm) for electronic noise of 900 electrons rms, while center of gravity did not. Our experimental efforts to apply analytical function fit to measured charge distributions did not improve the detector resolution due to the limited accuracy of the geometry of our first XS anodes, which has been substantially improved by some refinements of the manufacturing process.

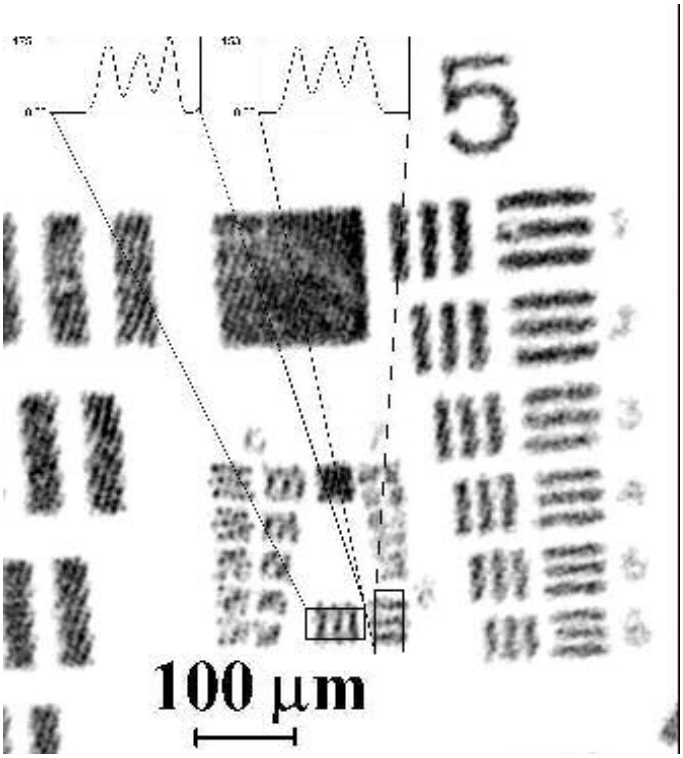

Fig. 5. Experimentally measured UV image of USAF resolution mask obtained with XS anode at detector gain of $6x10^5$ and electronic noise of ~500 e rms [3]. Chevron stack of 80:1 L/D MCP with 6 μm pores on ~7.2 μm centers is used in the measurements. The XS anode geometry is the same as the anode used in calculations of Fig.3. The image nonlinearity is due to geometric imperfections of fingers of our first XS anodes.

A. Accuracy of the Anode Geometry and Image Linearity

The linearity of images obtained with a cross strip anode was found to be strongly dependent on the accuracy of the anode geometry. There are technological limitations to the achievable accuracy of the anode geometry comprising a 3-dimensional structure. The accuracy of top electrodes is obviously most difficult to control as some geometric artifacts accumulate through the layers. In our modeling described in this section we shifted the boundaries of individual top electrodes by a given value and then calculated the images obtained with such anode. The bottom electrodes were assumed to have perfect geometric accuracy.

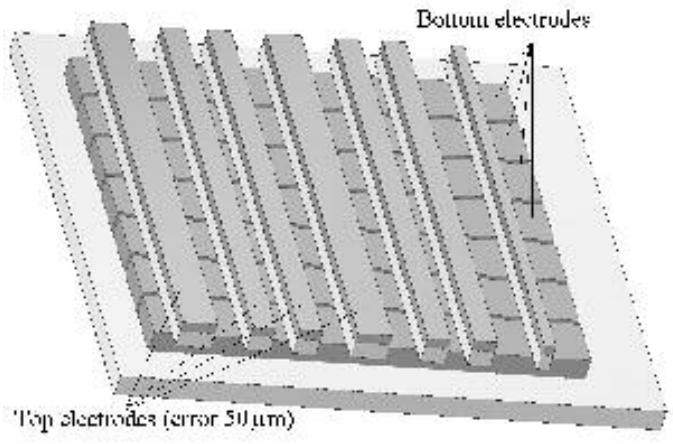

Fig. 6. The image of modeled XS anode with geometrical error Δ_{geom} of top electrodes equal to 50 μm. Anode period 0.5 mm, top and bottom electrodes ideally are 0.2 and 0.45 mm wide, respectively. The width of top electrodes changes between 0.1 and 0.3 mm and the center of each electrode can be shifted by 50 μm.

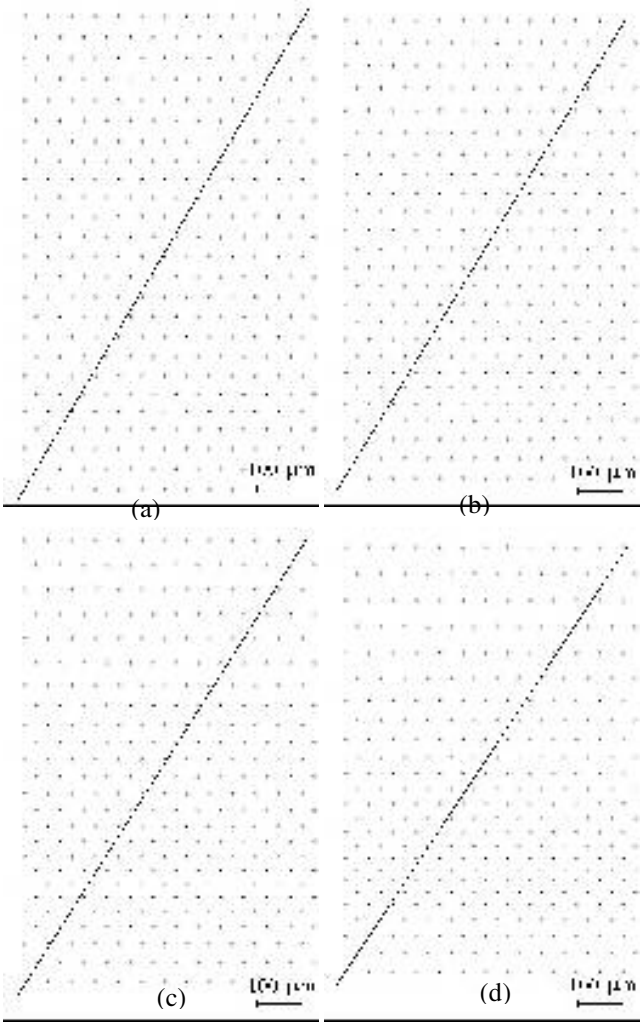

Fig. 7. The modeled images obtained with XS anode with different values of geometrical error Δ_{geom} of top electrodes: (a) 5 μm, (b) 25 μm, (c) 50 μm (anode shown in Fig. 6) and (d) 75 μm. An array of hexagonally packed holes on 50 μm centers is imaged. 500 photons per individual hole are modeled. Detector gain is 5×10^5 and electronic noise is 500 electrons rms.

The fragment of an anode shown in Fig. 6 corresponds to a Δ_{geom} = 50 μm inaccuracy of the anode electrodes. The left and right boundaries of each electrode were shifted (in a randomly chosen direction) by Δ_{geom} and the direction of the individual shifts was the same during calculations with different values of parameter Δ_{geom}. Both position of the electrode center and its width could be changed by these Δ_{geom} shifts, as seen in Fig. 6.

The images obtained with different values of parameter Δ_{geom} are shown in Fig. 7. Only distortions along the vertical axis are seen in these images. In reality the inaccuracies of top electrodes influence charge collection by bottom electrodes, but not vice versa, and we believe that the image distortions along the axis encoded by bottom electrodes to be not larger than along the other axis. An illumination through an array of hexagonally packed pinholes was selected as an input to the detector. Results of our calculations illustrate by how much the linearity of cross strip anode degrades as parameter Δ_{geom} is increased. With the help of our model we can determine now what should be the accuracy of the anode geometry in order to limit image distortions within a given value. At the same time it should be noted that these distortions are fixed and can be corrected by a proper detector calibration. We confirmed with the help of the model that the ~20 μm distortions of the images obtained with our initial cross strip anodes are indeed due to geometric inaccuracies. Some considerable efforts were invested in optimizing the manufacturing process, which led to a better geometric accuracy of our newest anodes.

IV. References

[1] O. H. W. Siegmund, A. S. Tremsin, J. V. Vallerga and J. Hull, "Cross strip imaging anodes for microchannel plate detectors", *IEEE Trans. Nucl. Sci.*, vol. 48, pp.430-434, 2001.

[2] O. H. W. Siegmund, A. S. Tremsin, J. V. Vallerga, R. Abiad and J. Hull, "High resolution cross strip anodes for photon counting detectors", *Nucl. Instrum. Methods*, vol.. A504, pp.177-181, 2003.

[3] A. S. Tremsin, O. H. W. Siegmund, J. V. Vallerga, J. S. Hull, R. Abiad, "Cross strip readouts for photon counting detectors with high spatial and temporal resolution", *IEEE Trans. Nucl. Sci.*, vol. 51, pp.1707-1711, 2004.

[4] A. S. Tremsin, O. H. W. Siegmund, "Spatial distribution of electron cloud footprints from microchannel plates: measurements and modelling", *Rev. Sci. Instr.* vol 70, pp.3282-3288, 1999.

[5] A. S. Tremsin, O. H. W. Siegmund, "Charge cloud asymmetry in detectors with biased MCPs", *Proc. SPIE*, vol.4497, pp.127-138, 2001.

[6] J. V Vallerga, O. H. W. Siegmund, J. Dalcomo, P. N Jelinsky, "High-resolution (<10-μm) photon-counting intensified CCD", *Proc. SPIE*, vol. 3019, pp. 156-167, 1997.

[7] S. H. Baik, S. K. Park, C. J. Kim, Y. S. Seo, Y. J. Kang, "New centroid detection algorithm for the Shack-Hartmann wavefront sensor", *Proc. SPIE*, vol. 4926, pp. 251-260, 2002.

[8] A. S. Tremsin, J. V. Vallerga, O. H. W. Siegmund, J. S. Hull, "Centroiding algorithms and spatial resolution of photon counting detectors with cross strip anodes", *Proc. SPIE*, vol. 5164 pp. 113-124, 2003.